

## Effect of Shear Stresses on Failure of Fibrous Composite Materials Accounting for Nonlinear Material Behavior

Ghazi Abu-Farsakh

Professor of Structural Engineering, Civil Engineering Department, Jordan University of Science and Technology.  
E-Mail: ghazi@just.edu.jo

### ABSTRACT

Variation of shear stresses  $\tau_{xy}$  on failure behavior of different composite materials was investigated for two types of composites; Boron-Epoxy Narmco 5505 and Carbon-Epoxy AS4 (3501-6). The effect of material nonlinearity on failure behavior of unidirectional fibrous composite laminates was considered for several fiber-orientation angles;  $\Theta=15, 30, 45, 60$  and  $75$  degrees. An energy-based nonlinear material model was adopted to predict the mechanical properties of a unidirectional composite lamina. A compatible failure criterion for nonlinear composite materials was utilized which incorporates the material model into the failure criterion. The resulting failure envelopes were compared for all the cases.

**KEYWORDS:** Shear stress, Failure envelope, Composite material, Nonlinear behavior, Fiber-orientation.

### INTRODUCTION

A fibrous composite material is composed of long fibers embedded in a matrix material to form what is known a lamina or a ply. The fibers are presumed to be strong and stiff while the matrix has low strength, low stiffness and low weight. A composite material is designed to attain certain main advantages, such as: high strength/weight, high stiffness/weight, corrosion resistance,... etc.

In two-dimensional plane stress state, unidirectional fibrous composite materials behave as generally orthotropic materials, where the in-plane principal material axes may not coincide with the laminate geometric axes, hence allowing the lamina in-plane normal stresses ( $\sigma_x, \sigma_y$ ) and shear stress ( $\tau_{xy}$ ) to be coupled in what is known as *coupling behavior*. This means that normal stresses ( $\sigma_x, \sigma_y$ ) will cause shear strain ( $\gamma_{xy}$ ) and shear stress ( $\tau_{xy}$ ) will cause normal

strains ( $\epsilon_x, \epsilon_y$ ).

In macro-mechanics, the composite material is presumed homogeneous and the material mechanical properties are dealt with as averaged apparent properties. The macro-mechanical properties of a composite material lamina of orthotropic construction are specified as:  $E_1, E_2, G_{12}$  and  $\nu_{12}$  in the principal material directions 1 and 2. These material properties are also known as the engineering material constants that have a physical and more direct meaning than stiffness and compliance coefficients. Such constants can be measured directly in uniaxial tension, compression or pure shear tests.

The lamina mechanical properties can be determined experimentally or using micro-mechanical approaches (Jones, 1975) which utilize the mechanical properties of composite material constituents (fibers and matrix). There are two basic approaches to micro-mechanics of composite materials: mechanics of materials and elasticity.

Considerable work has been carried out on micro-mechanical approaches (Jones, 1975; Hashin and Rozen, 1964; Willis, 1977; Hashin, 1979; Hashin, 1983; Sun and Vaidya, 1994). A major objective of such work is to determine the elastic moduli (stiffnesses or compliances) of the composite material in terms of its constituent materials; fibers and matrix. An additional objective is to estimate the strength of a composite material in terms of strength of its constituents. Several material models have been proposed to model the nonlinear behavior of composite materials (Frost, 1990; Gibson, 1994) which treats the composite material on a macroscopic scale.

Several failure criteria were implemented in the literature using different approaches:

- Mechanics approach (stress or strain);
- Energy-based criteria;
- Fracture mechanics approach;
- Plasticity approach;
- Damage mechanics approach.

A comprehensive description of such approaches can be found in (Donadon et al., 2009). In their work, Donadon et al. (2009) and Donadon et al. (2008) presented an interactive failure criterion which incorporates the strain rate effect in in-plane shear behavior and utilizes damage evolution laws for better prediction of damage initiation and progress under multi-axial stress states.

In the present research work, an energy-based nonlinear material model (Abu-Farsakh, 1989) is adopted to predict the mechanical properties of a unidirectional composite lamina. A related failure criterion for nonlinear composite materials was developed in (Donadon et al., 2008). In order to account for the nonlinear effect of the material, the material model is incorporated in the failure criterion.

### OBJECTIVES AND SCOPE

The main objective of the present research is aimed to obtain the effect of material nonlinearity on the failure behavior of unidirectional fibrous composite

laminates. Variation of shear stresses  $\tau_{xy}$  on the failure behavior of different composite materials will be considered accounting for linear and nonlinear material effects. The resulting failure envelopes will be compared for all the cases.

### MODEL FORMULATION

The basic formulation (Donadon et al., 2008) of the failure model is dependent on an energy-based concept such that:

$$\frac{U_1}{U_{1\max}} + \frac{U_2}{U_{2\max}} + \frac{U_{12}}{U_{12\max}} = 1 \quad \dots (1)$$

where,

$U_1, U_{1\max}$  : Strain energy density and its corresponding maximum value in the fiber-direction.

$U_2, U_{2\max}$  : Strain energy density and its corresponding maximum value in the transverse direction.

$U_{12}, U_{12\max}$  : In-plane shear strain energy density and its corresponding maximum value.

The energy terms are determined assuming an equivalent linear elastic system. For more details on the nonlinear material model, consult (Donadon et al., 2009). The secant mechanical properties are used in the modeling process. See Fig. 1 for terminology.

The nonlinear mechanical properties are expressed as:

$$M_i = M_o \left( 1 - B_i (\bar{U}_p)^{C_i} + D_i (\bar{U}_p) \right) \quad \dots (2)$$

where,

$M_i, M_o$ : Secant and tangential mechanical property.

$B_i, C_i, D_i$ : Material property constants for mechanical property  $i$ .

Three mechanical properties are expressed using Eq. 2;  $E_1, E_2$  and  $G_{12}$ . The initial values of mechanical properties and the corresponding material constants are as indicated in Tables 1 to 3. The plastic strain energy term  $(\bar{U}_p)$  is normalized as:

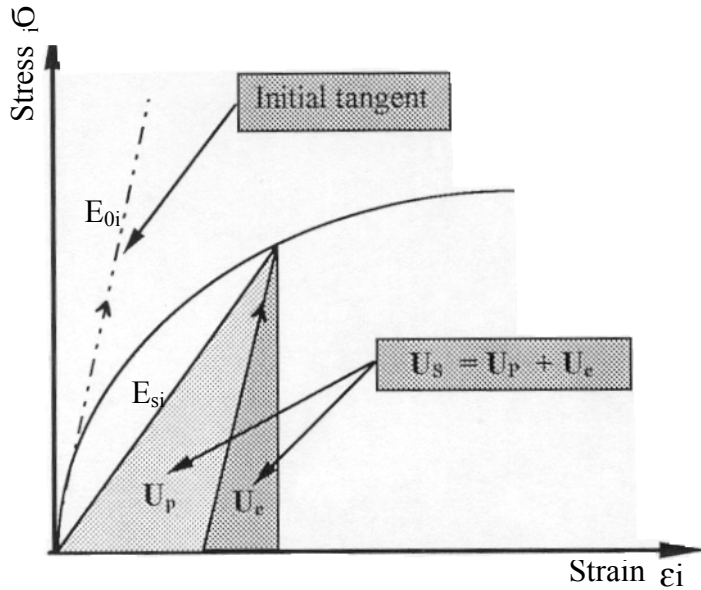


Figure 1: Typical non-linear stress-strain curve for the  $i^{th}$  mechanical property showing the strain energy density terms

$$(\bar{U}_p) = \frac{U_p}{U_o} = \frac{U_s - U_e}{U_o} \quad \dots (3)$$

For in-plane stress case, the total secant strain energy density ( $U_s$ ) may be expressed in terms of laminate geometric axes x & y as:

$$U_s = \frac{1}{2} (\sigma_x \epsilon_x + \sigma_y \epsilon_y + \tau_{xy} \gamma_{xy}) \quad \dots (4)$$

Or alternatively, it can be expressed in terms of principal material directions (1 & 2) as:

$$U_s = \frac{1}{2} \left( \frac{\sigma_1^2}{E_1} + \frac{\sigma_2^2}{E_2} + \frac{\tau_{12}^2}{G_{12}} \right) \quad \dots (5)$$

where,  $E_1$ ,  $E_2$  and  $G_{12}$  are the secant moduli at each stress level.

Similarly, the initial elastic moduli  $E_{o1}$ ,  $E_{o2}$  and  $G_{o12}$  can be used to obtain the elastic strain energy density, such that:

$$U_e = \frac{1}{2} \left( \frac{\sigma_1^2}{E_{o1}} + \frac{\sigma_2^2}{E_{o2}} + \frac{\tau_{12}^2}{G_{o12}} \right) \quad \dots (6)$$

The plastic strain energy density ( $U_p$ ) is obtained (as shown in Fig. 1) as:

$$U_p = U_s - U_e \quad \dots (7)$$

The term ( $U_o$ ) is used to normalize the plastic strain energy density, and it is usually taken equal to unity (i.e., 1 MPa).

### MODEL VALIDATION

In order to validate the present approach, two fibrous composite materials were considered: Boron-epoxy Narmco 5505 and Carbon-epoxy AS4 (3501-6). The basic material properties are taken from (Soden et al., 1998; Soden et al., 2002; Cole and Pipes, 1973) as indicated in Tables 1 and 2. Applications were carried out using off-axis coupon specimens loaded in the uniaxial x-direction. The in-plane principal material directions are the longitudinal fiber 1-direction and transverse to fiber 2-direction. The fiber orientation  $\Theta$

angle is the angle between the x-axis and the longitudinal fiber 1-direction. For each composite

material, several fiber-orientation angles were considered.

**Table 1. Material mechanical properties of Boron-Epoxy Narmco 5505 (basic data extracted from (Cole and Pipes, 1973))**

MATERIAL PROPERTIES	MATERIAL CONSTANTS					
	$E_o$ (MPa)	$B_i$	$C_i$	$D_i$	$LSE$	SP
$E_1$ (MPa)	$2.0752 \times 10^5$	0	1	0	-	-
$E_2$ (MPa)	$1.9787 \times 10^4$	0.213789	0.329364	-7.64104	0.000145	2,4,5
$G_{12}$ (MPa)	$5.5155 \times 10^3$	0.924308	0.405749	0.217495	0.000311	2,5,7
$\sigma_{1max}$ (MPa)	1341					
$\epsilon_{1max}$	$6.525 \times 10^{-3}$					
$\sigma_{2max}$ (MPa)	53.776					
$\epsilon_{2max}$	$3.18 \times 10^{-3}$					
$\tau_{12max}$ (MPa)	64.118					
$\gamma_{12max}$	$31.6 \times 10^{-3}$					
$\nu_{12}$	0225					

Two sets of results were obtained. The first set includes a comparison between the predicted nonlinear stress-strain curve using the nonlinear material model (Eq. 2) and the predicted failure model (Eq. 2) which is represented as a single failure point. The second set includes a comparison between several in-plane shear stresses ( $\tau_{xy}$ ) showing the effect of varying the shear stress values from zero to a maximum value at failure. For each set of failure envelopes, the in-plane stresses  $\sigma_x$  and  $\sigma_y$  are kept constant while changing the values of shear stress  $\tau_{xy}$ .

### *Non-linear Stress-Strain Model*

#### **1. Boron-Epoxy Narmco 5505**

The basic stress-strain relations in the principal material directions are obtained from (Cole and Pipes, 1973). The material property constants which appear in Eq. 2 are obtained using a special computer program (MCOMP) coded using Window-based Visual Basic computer language. Boron-epoxy composite material is linear in the fiber direction-1 (Fig. 2) but slightly nonlinear transverse to fiber direction 2 (Fig.3). The

considered sampling points for  $\sigma_2$ - $\varepsilon_2$  relationship are 2, 4 and 5 which correspond to minimum least- square-fitting (LSE) of 0.000145. On the other hand, shear-stress shear-strain ( $\tau_{12}, \gamma_{12}$ ) behavior (Fig. 4) is highly nonlinear with optimum sampling points 2, 5 and 7 (LSE=0.000311). The obtained material constants  $B_i, C_i$  and  $D_i$  are as indicated in Table 1 for each nonlinear property. Maximum stress and strain values in the principal material directions are also as indicated in Table 1.

Several uniaxial off-axis coupon specimens were considered using different fiber-orientation angles;

$\Theta=15^\circ, 30^\circ, 45^\circ, 60^\circ$  and  $75^\circ$ . Predicted stress-strain curves are shown in Figs. 5 to 9 according to material model Eq.2 along with predictions from the failure model (Eq. 1). As indicated in Table 2, a maximum absolute difference of 6% in the stress- $\sigma_x$  between the two models is obtained at  $\Theta=15^\circ$ , whilst the maximum absolute difference of 8.9% in strain- $\varepsilon_x$  corresponds to  $\Theta=45^\circ$ . The reason behind this is the high nonlinear behavior in shear response which is greatly affected by the adopted shear test or method of prediction of shear response (Cole and Pipes, 1973).

**Table 2. Stress-strain results for Boron-Epoxy Narmco 5505**

Orientation Angle ( $\Theta^\circ$ )	Predicted Model		Failure Model	
	$\sigma_x$ (MPa)	$\varepsilon_x$ ( $\times 10^3$ )	$\sigma_x$ (MPa)	$\varepsilon_x$ ( $\times 10^3$ )
15	235.93	7.875	250.9	8.259
30	134.97	11.342	135.4	10.48
45	94	8.641	93.91	7.938
60	69.64	5.523	69.58	5.101
75	57.3	3.735	57.37	3.614

**2. Carbon-Epoxy AS4 (3501-6)**

The basic stress-strain data in the principal material direction (1 & 2) are obtained from (Soden et al., 1998; Soden et al., 2002) (as illustrated in Figs. 15 to 17). The material property constants  $B_i, C_i$  and  $D_i$  are as indicated in Table 3 for each nonlinear property. The stress-strain relationships were linear in the fiber and transverse directions, while the in-plane shear behavior was nonlinear. The sampling points for shear were selected at points 2, 6 and 12 with LSE of 0.000017 as indicated in Table 3. Also, points of maximum stresses and strains in the corresponding principal material directions are exhibited in Table 3.

The various uniaxial off-axis coupon specimens were obtained using different fiber-orientation angles;  $\Theta=20^\circ, 30^\circ, 45^\circ, 60^\circ$  and  $75^\circ$ . Predicted stress-strain curves are shown in Figs. 18 to 22 according to the

material model presented in Eq.2 along with predictions from the failure model (Eq. 1). As indicated in Table 4, a maximum absolute difference of 8.1% in the stress- $\sigma_x$  between the two models is obtained at  $\Theta=20^\circ$ , whilst the maximum absolute difference of 5.9% in strain- $\varepsilon_x$  occurs at the same angle. This may be attributed to the high effect of nonlinear shear behavior at this angle.

**Failure Shear-Envelopes**

**1. Boron-Epoxy Narmco 5505**

1. Several in-plane shear stresses ( $\tau_{xy}$ ) showing the effect of varying the shear-stress values from 0, 20, 40, 60 up-to a maximum value at failure ( $\tau_{xy})_u = 64.118MPa$  are exhibited in Figs. 10 to 14. For each set of failure envelopes, the in-plane stresses  $\sigma_x$  and  $\sigma_y$  are kept constant while changing the values

of shear stress  $\tau_{xy}$ . As the orientation-angle  $\Theta$  is increased from 15°, 30°, 45°, 60° up-to 75°, the resulting sets of failure envelopes rotate accordingly in a counter-clock-wise sense in a systematic manner. The envelopes start to stretch in two perpendicular axes as the orientation-angle is increased from  $\Theta=0^\circ$  up-to

$\Theta=45^\circ$ . At angles ( $\Theta>45^\circ$ ), the process is reversed with respect to these two perpendicular directions, where the axes start to widen in one direction and become narrow in the perpendicular direction. This method can be described as Narrowing-Widening-Stretching (NWS) mechanism.

**Table 3. Material mechanical properties of Carbon-Epoxy AS4 (3501-6)**  
(basic data extracted from (Soden et al., 1988; Soden et al., 2002))

MATERIAL PROPERTIES	MATERIAL CONSTANTS					
	$E_o$ (MPa)	$B_i$	$C_i$	$D_i$	LSE	SP
$E_1$ (MPa)	1.4496 X10 <sup>5</sup>	0	1	0	-	-
$E_2$ (MPa)	1.0597x10 <sup>4</sup>	0	1	0	-	-
$G_{12}$ (MPa)	7.9286x10 <sup>3</sup>	1.467094	0.604288	1.031930	0.000017	2,6,12
$\sigma_{1\max}$ (MPa)	2268.3					
$\varepsilon_{1\max}$	15.2x10 <sup>-3</sup>					
$\sigma_{2\max}$ (MPa)	59.981					
$\varepsilon_{2\max}$	5.6x10 <sup>-3</sup>					
$\tau_{12\max}$ (MPa)	71.702					
$\gamma_{12\max}$	13.0x10 <sup>-3</sup>					
$\nu_{12}$	027					

**Table 4. Stress-strain results for Carbon-Epoxy AS4 (3501-6)**

Orientation Angle ( $\Theta^\circ$ )	Predicted Model		Failure Model	
	$\sigma_x$ (MPa)	$\varepsilon_x$ (x10 <sup>3</sup> )	$\sigma_x$ (MPa)	$\varepsilon_x$ (x10 <sup>3</sup> )
20	191.77	4.775	208.6	5.075
30	141.97	5.951	141.6	5.629
45	95.95	6.158	96.06	5.836
60	72.14	5.749	73.65	5.743
75	62.79	5.661	62.86	5.663

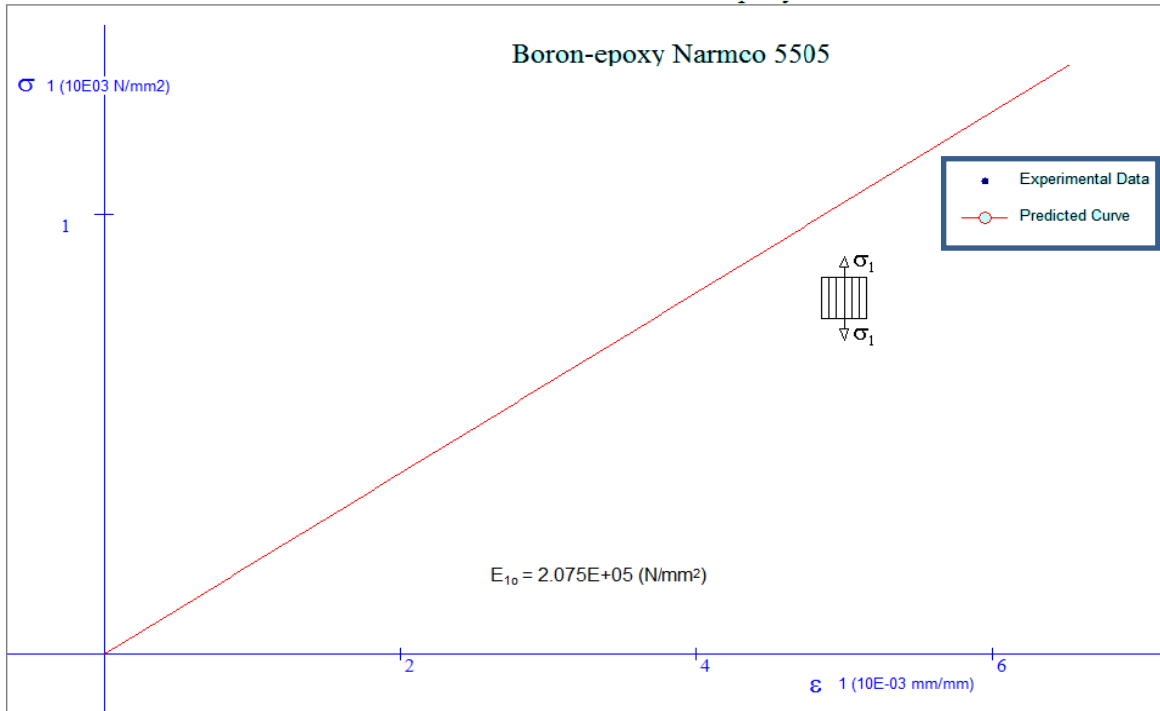


Figure 2: Stress-strain diagram for Boron-Epoxy in the principal material 1-direction

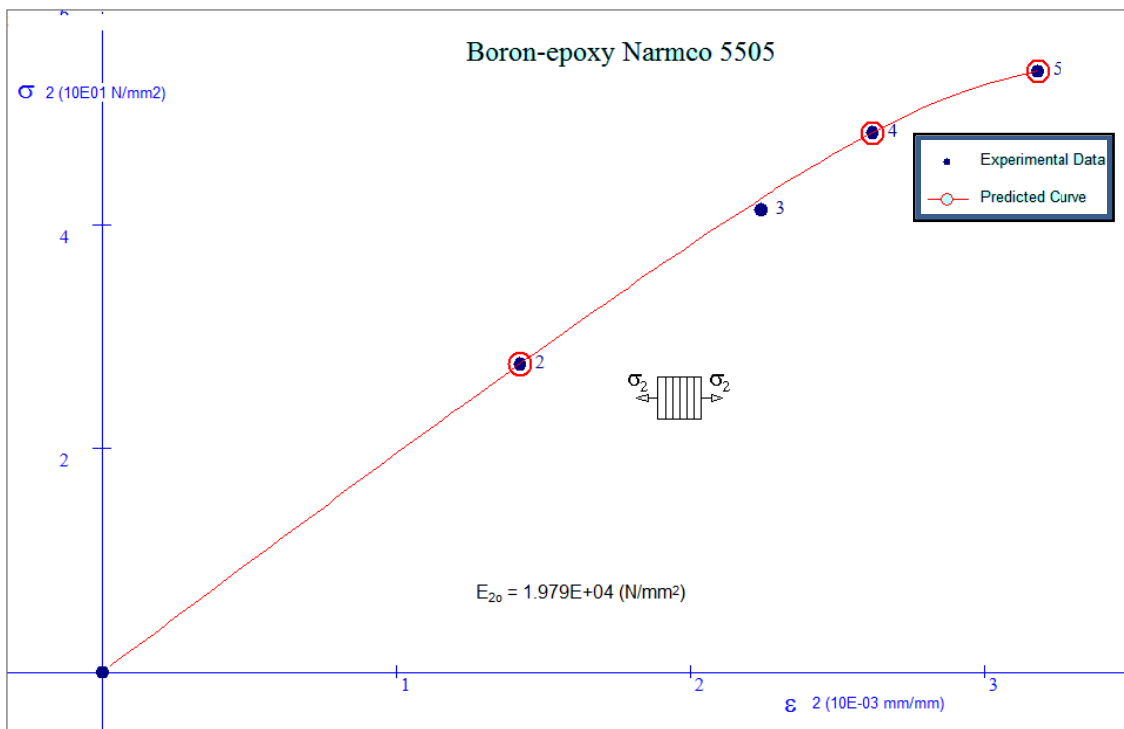


Figure 3: Stress-strain diagram for Boron-Epoxy in the principal material 2-direction

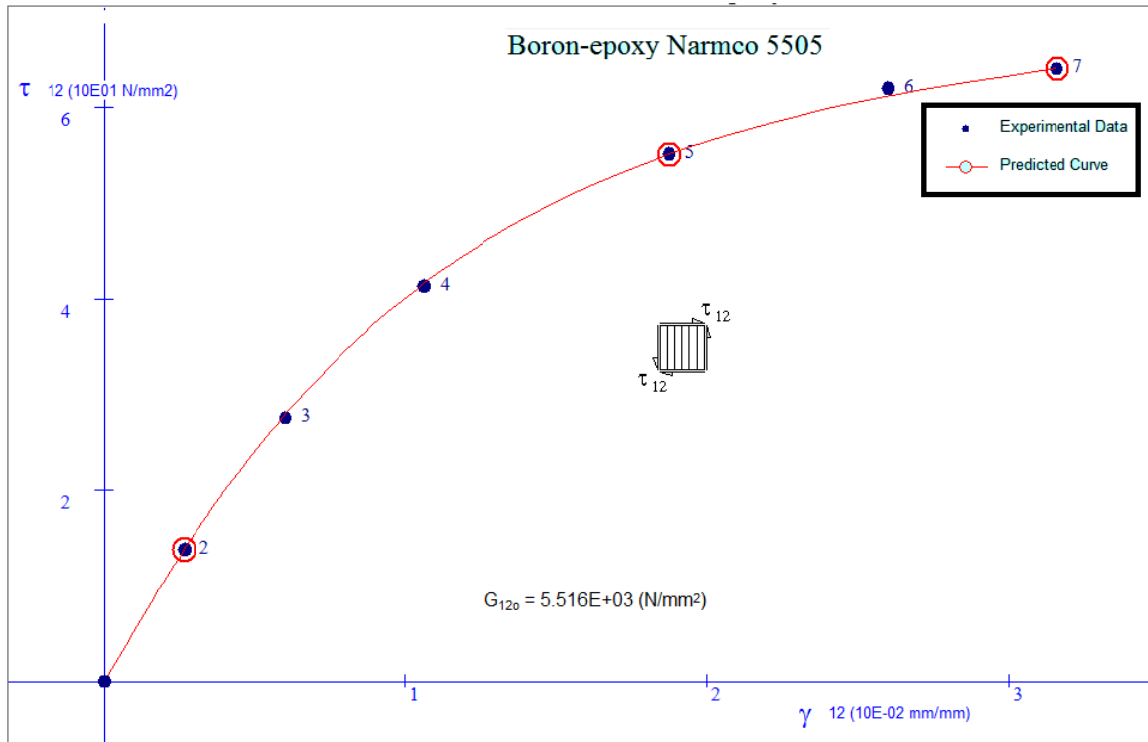


Figure 4: In-plane shear stress-strain diagram for Boron-Epoxy in the principal material 12-direction

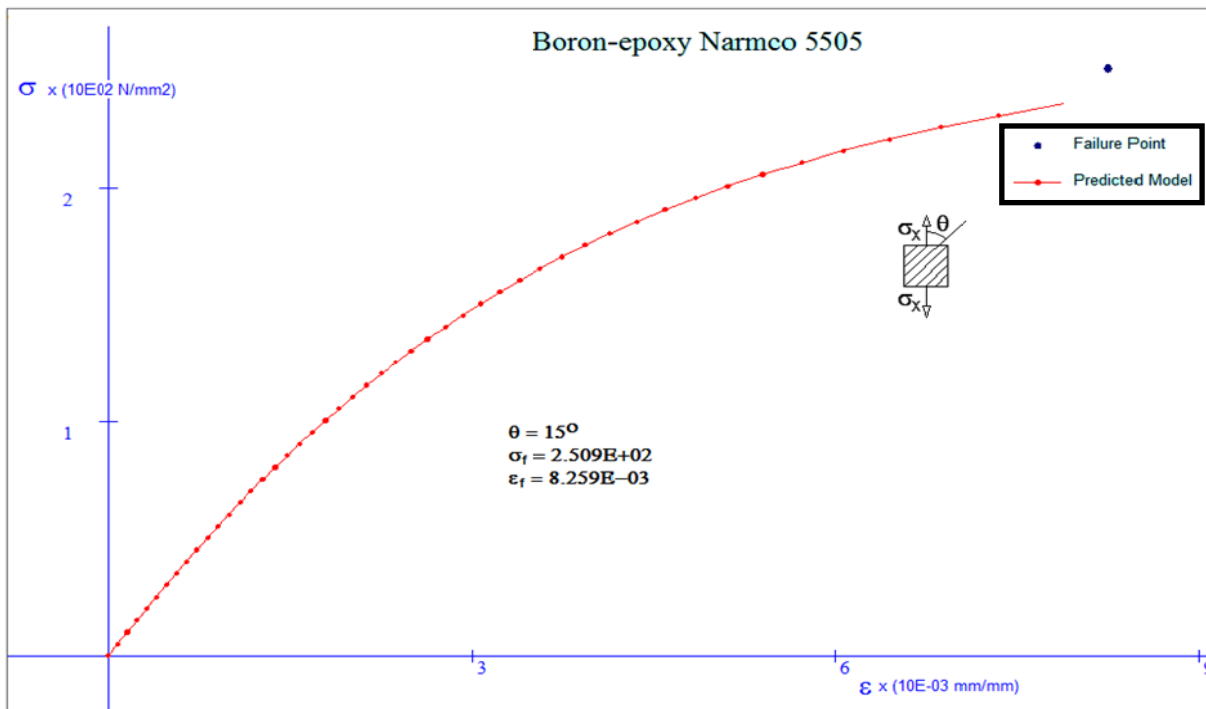


Figure 5: Stress-strain diagram for Boron-Epoxy in the x-direction at  $\Theta = 15$  degrees



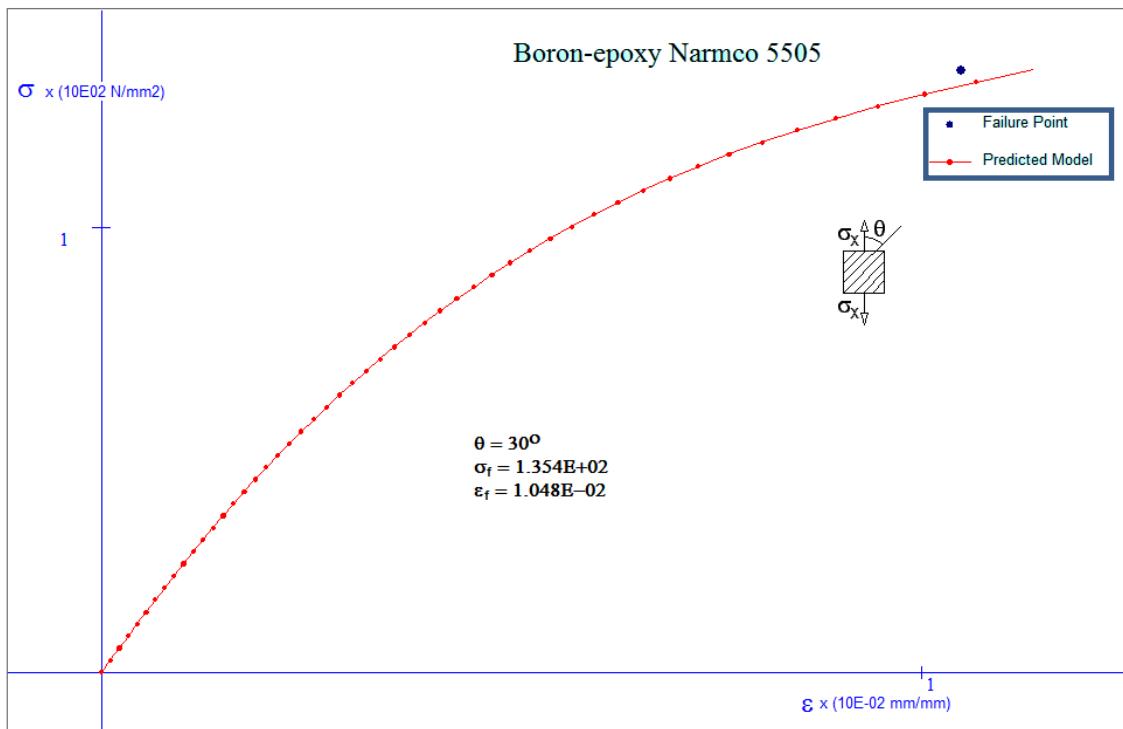


Figure 6: Stress-strain diagram for Boron-Epoxy in the x-direction at  $\Theta=30$  degrees

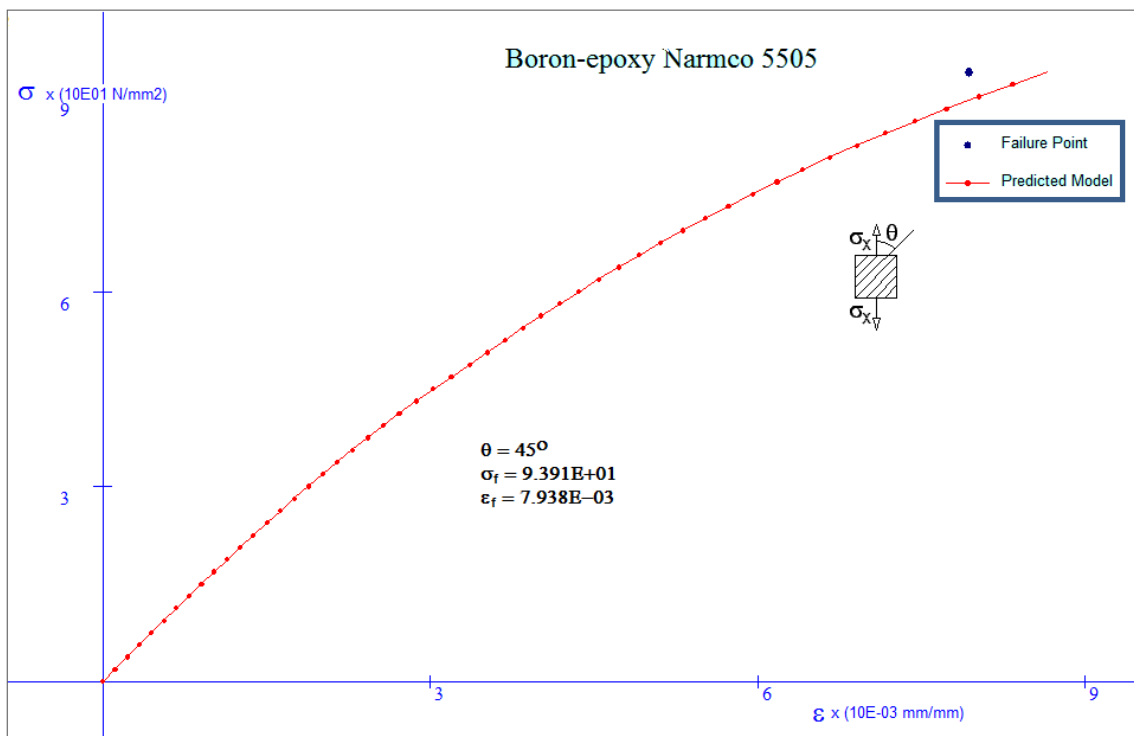


Figure 7: Stress-strain diagram for Boron-Epoxy in the x-direction at  $\Theta=45$  degrees

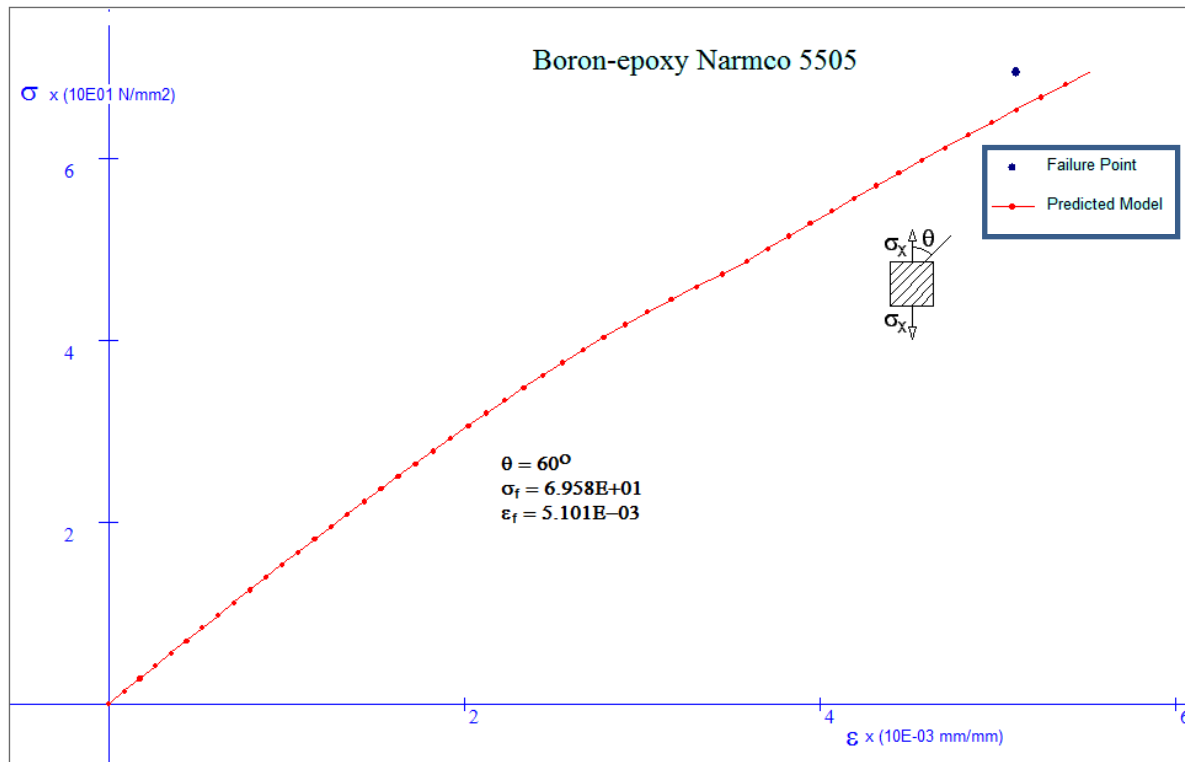


Figure 8: Stress-strain diagram for Boron-Epoxy in the x-direction at  $\Theta=60$  degrees

## 2. Carbon-Epoxy AS4 (3501-6)

The effect of varying the in-plane shear stresses ( $\tau_{xy}$ ) from 0, 20, 40, 60 up-to a maximum value at failure  $(\tau_{xy})_u = 71.702MPa$  is illustrated in Figs. 23 to 27. As mentioned earlier, the in-plane stresses  $\sigma_x$  and  $\sigma_y$  are kept constant for each set of failure envelopes. The orientation-angle  $\Theta$  is varied from  $20^\circ$ ,  $30^\circ$ ,  $45^\circ$ ,  $60^\circ$  up-to  $75^\circ$ . The resulting failure envelopes are similar in approach as those obtained for Boron-Epoxy composite according to NWS-mechanism.

## CONCLUSIONS

Two main conclusions can be drawn from the present research:

- A comprehensive description of the nonlinear material model is carried out showing the detailed steps of performing a successful comparison between model prediction and end-point failure-model prediction. Two fibrous composite materials are considered in the validation process; Boron-Epoxy Narmco 5505 and Carbon-Epoxy AS4 3501-6. The accomplished results were, in most cases, of excellent agreement between the two methods. The maximum absolute discrepancy between predicted stresses was 8.1% at  $\Theta=20^\circ$  for Carbon-Epoxy AS4 3501-6, whilst the maximum absolute difference in strains was 8.9% at  $\Theta=45^\circ$  for Boron-Epoxy Narmco 5505.
- The effect of varying the in-plane shear stresses

( $\tau_{xy}$ ) in five-steps is obtained from zero up-to a maximum shear value at failure, while the in-plane normal stresses  $\sigma_x$  and  $\sigma_y$  are kept constant for each set of failure envelopes. The orientation-angle  $\Theta$  is varied from  $15^\circ$  up-to  $75^\circ$ . The resulting failure envelopes rotate in a counter-clock-wise sense in a systematic and specific manner as the orientation-angle is increased. The method was

described as Narrowing-Widening-Stretching (NWS) mechanism.

**Acknowledgement**

The author would like to express his great gratitude for Jordan University of Science and Technology for their funding support during my sabbatical year 2011-2012 spent at Jerash University in Jordan.

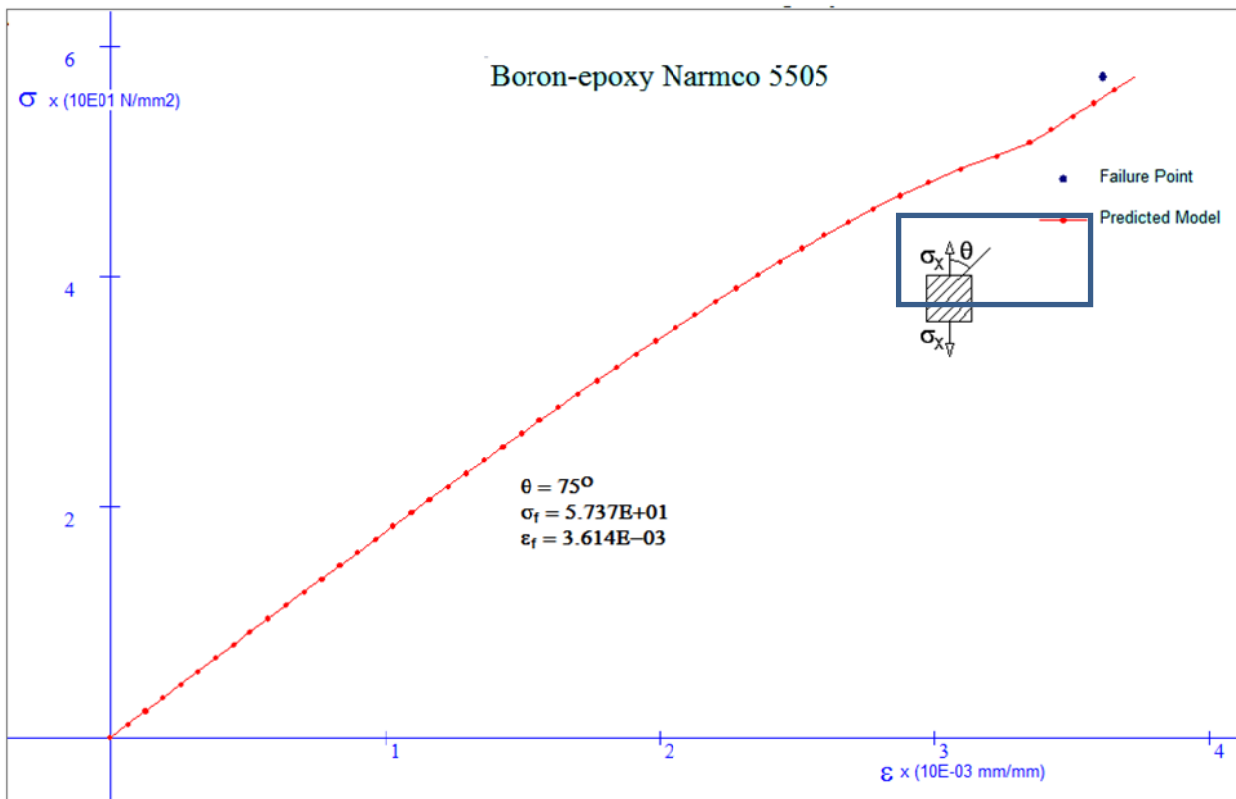


Figure 9: Stress-strain diagram for Boron-Epoxy in the x-direction at  $\Theta=75$  degrees

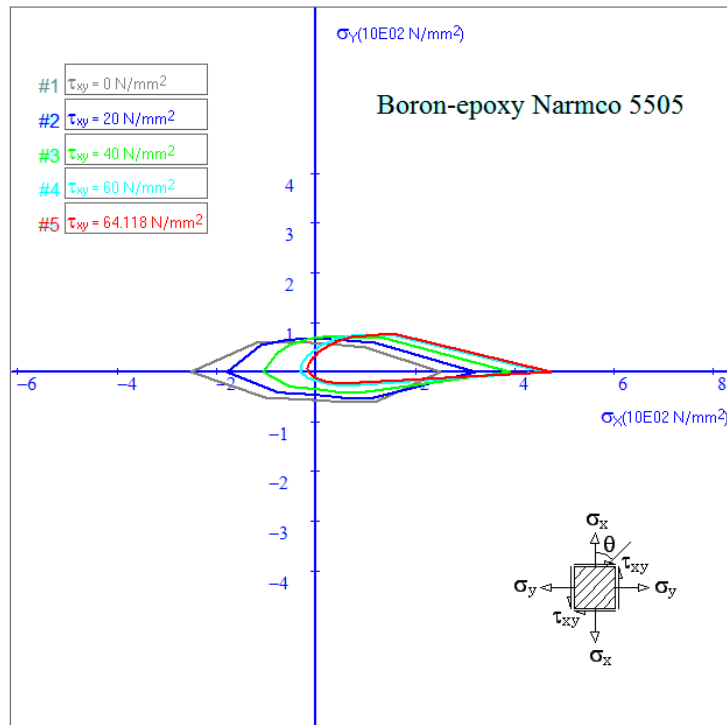


Figure 10: Failure envelopes for Boron-Epoxy for various in-plane shear stresses at  $\theta=15$  degrees

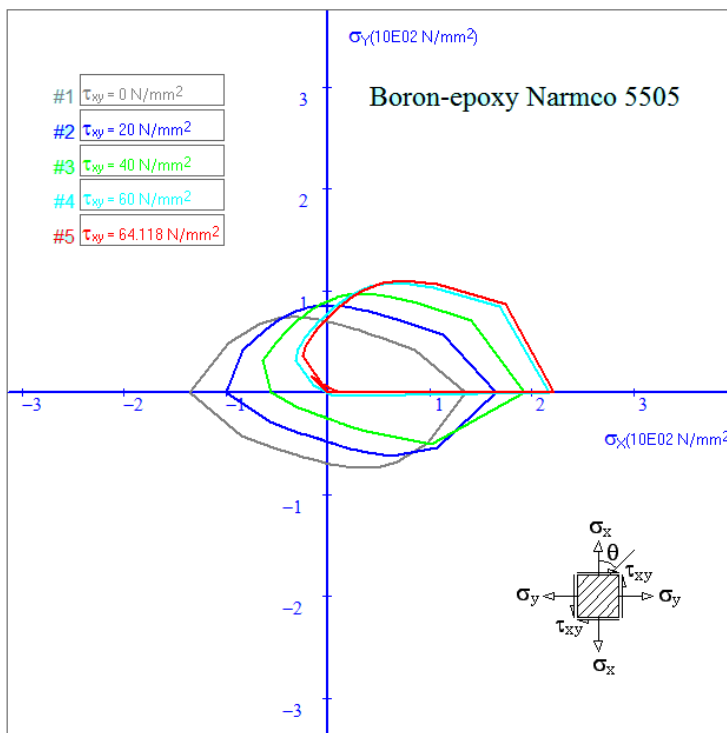


Figure 11: Failure envelopes for Boron-Epoxy for various in-plane shear stresses at  $\theta=30$  degrees

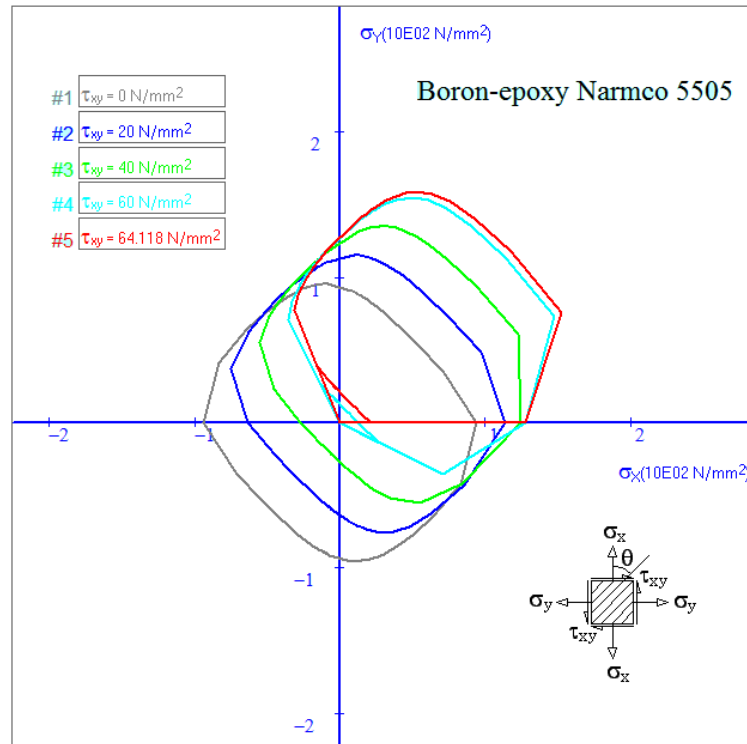


Figure 12: Failure envelopes for Boron-Epoxy for various in-plane shear stresses at  $\theta=45$  degrees

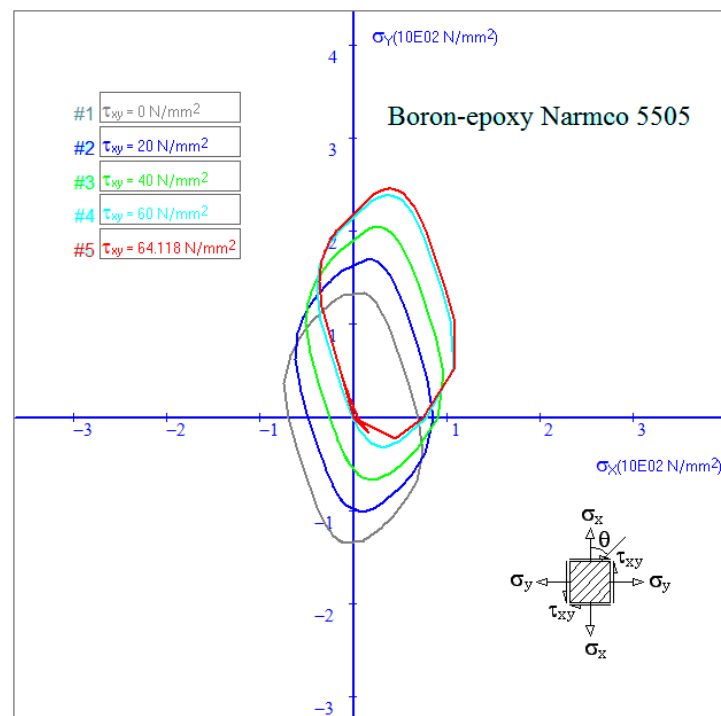


Figure 13: Failure envelopes for Boron-Epoxy for various in-plane shear stresses at  $\theta=60$  degrees

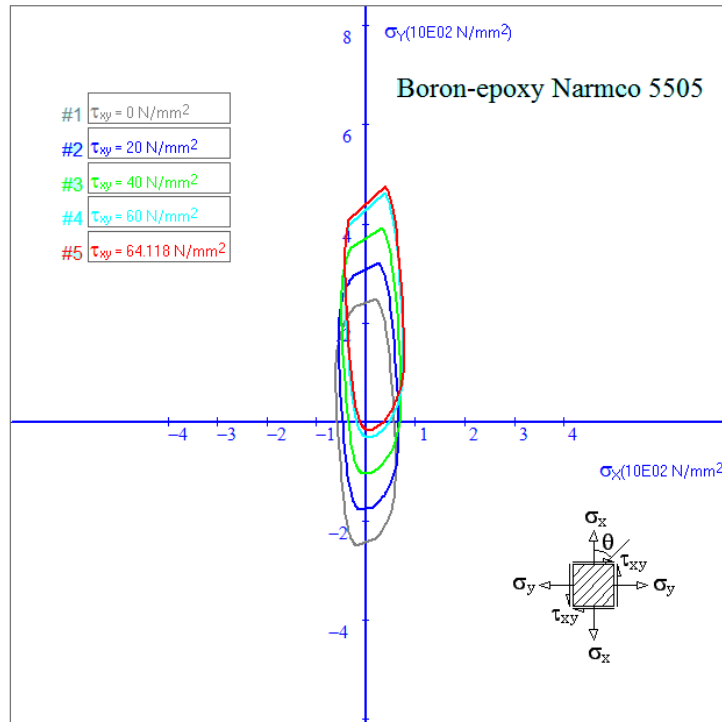


Figure 14: Failure envelopes for Boron-Epoxy for various in-plane shear stresses at  $\theta=75$  degrees

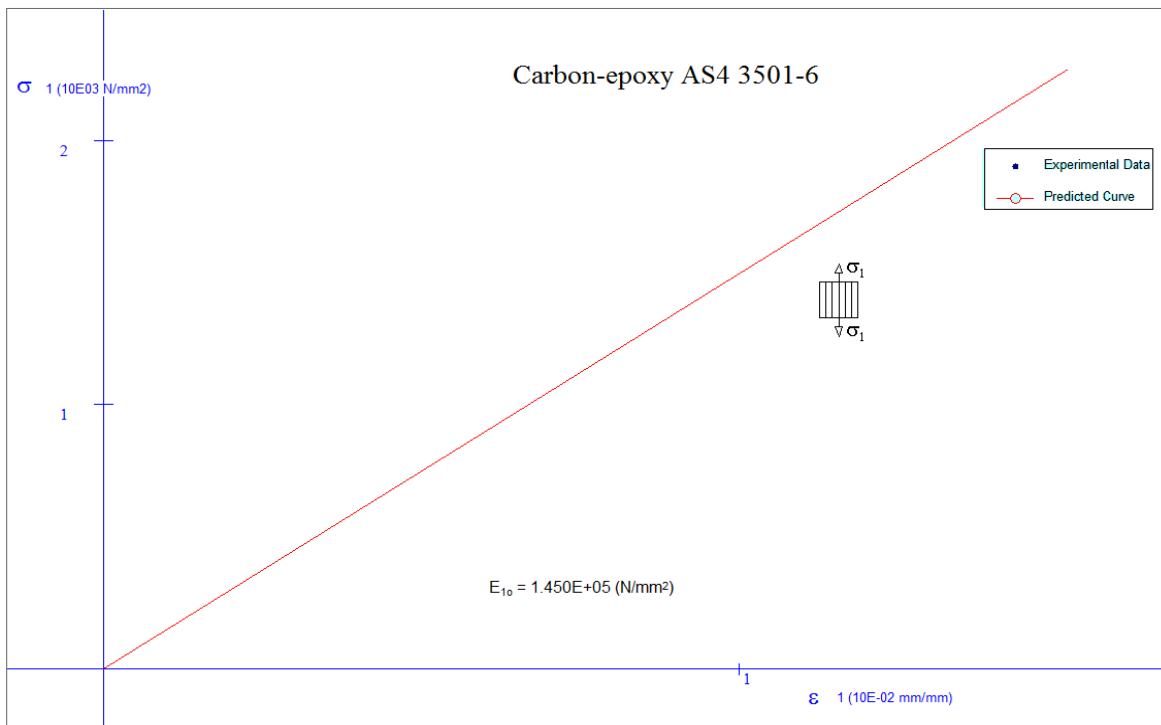


Figure 15: Stress-strain diagram for Carbon-Epoxy in the principal material 1-direction

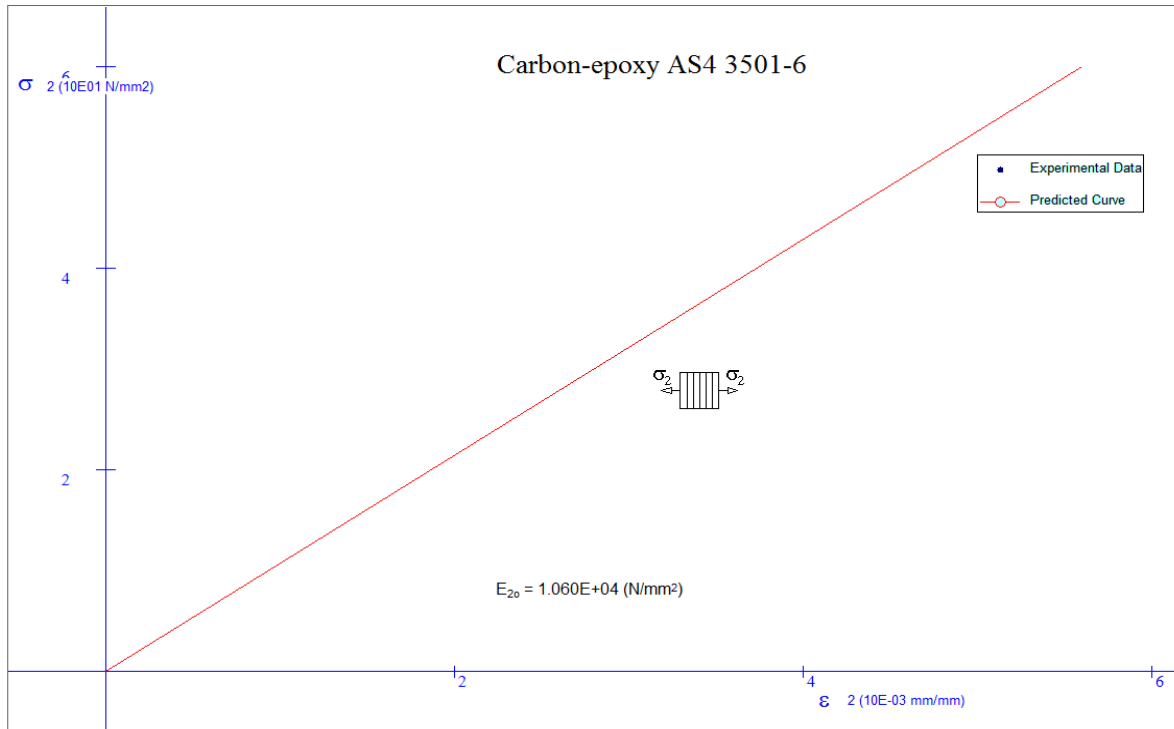


Figure 16: Stress-strain diagram for Carbon-Epoxy in the principal material 2-direction

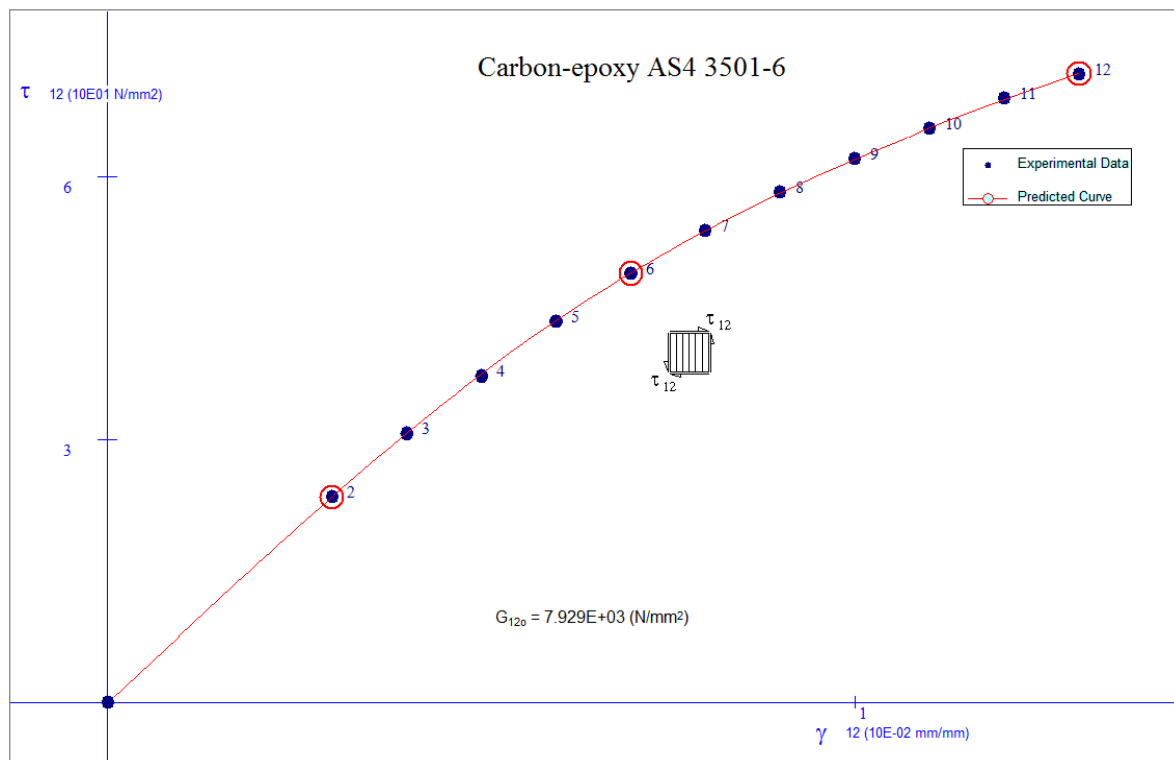


Figure 17: In-plane shear stress-strain diagram for Carbon-Epoxy in the principal material 12-direction

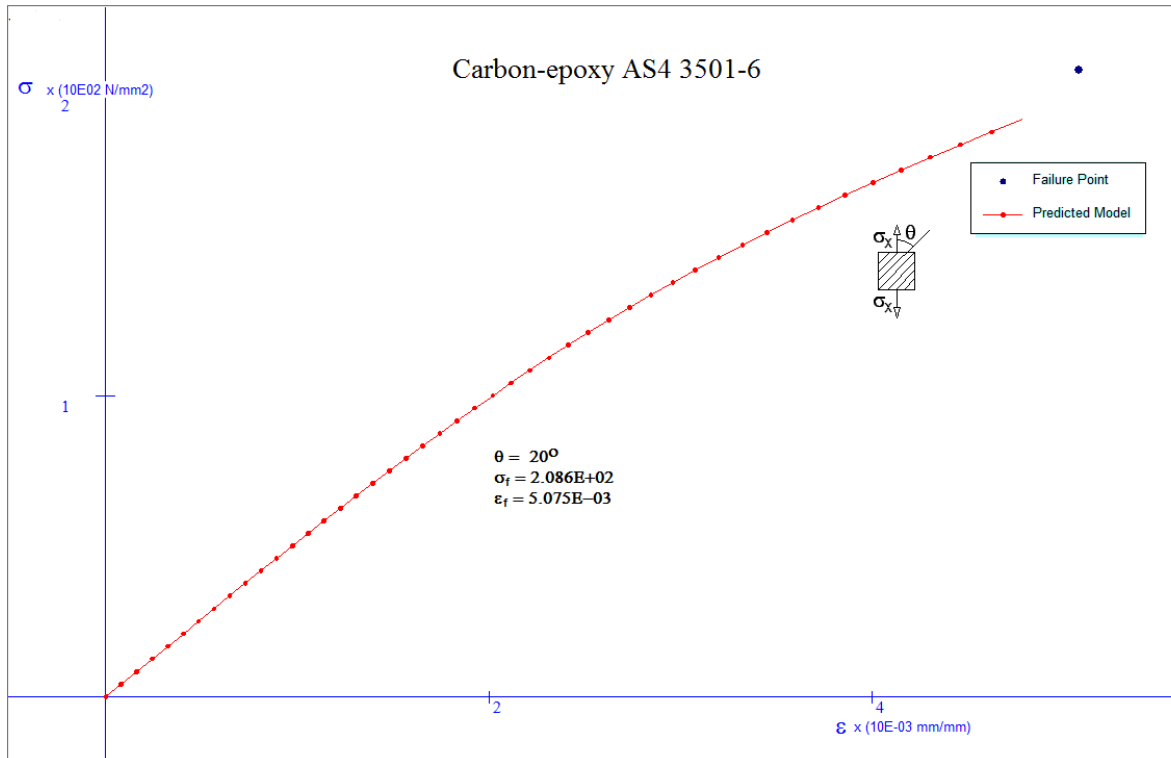


Figure 18: Stress-strain diagram for Carbon-Epoxy in the x-direction at  $\Theta=20$  degrees

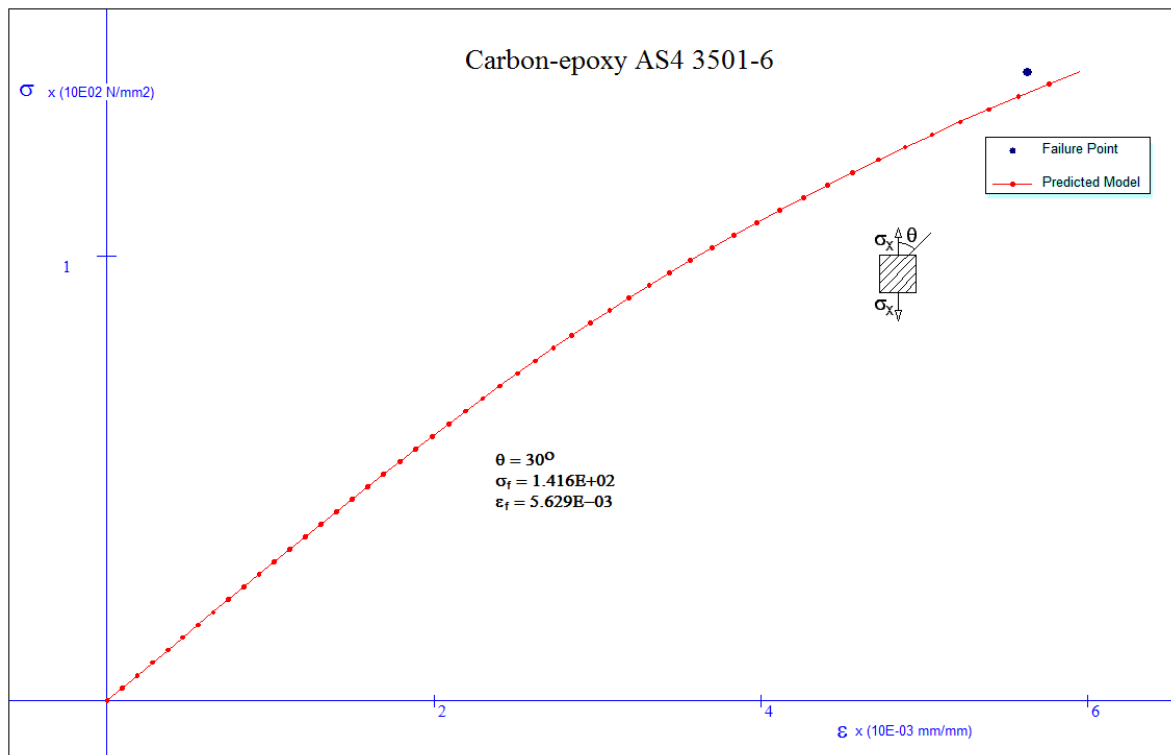


Figure 19: Stress-strain diagram for Carbon-Epoxy in the x-direction at  $\Theta=30$  degrees



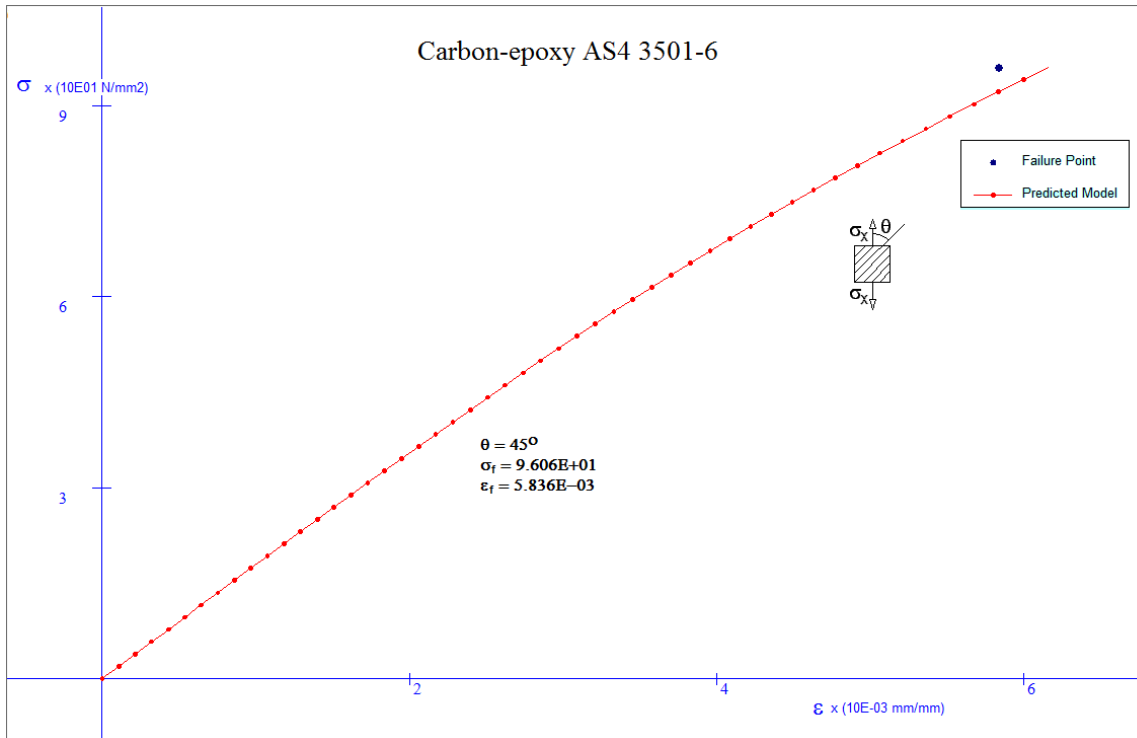


Figure 20: Stress-strain diagram for Carbon-Epoxy in the x-direction at  $\Theta=45$  degrees

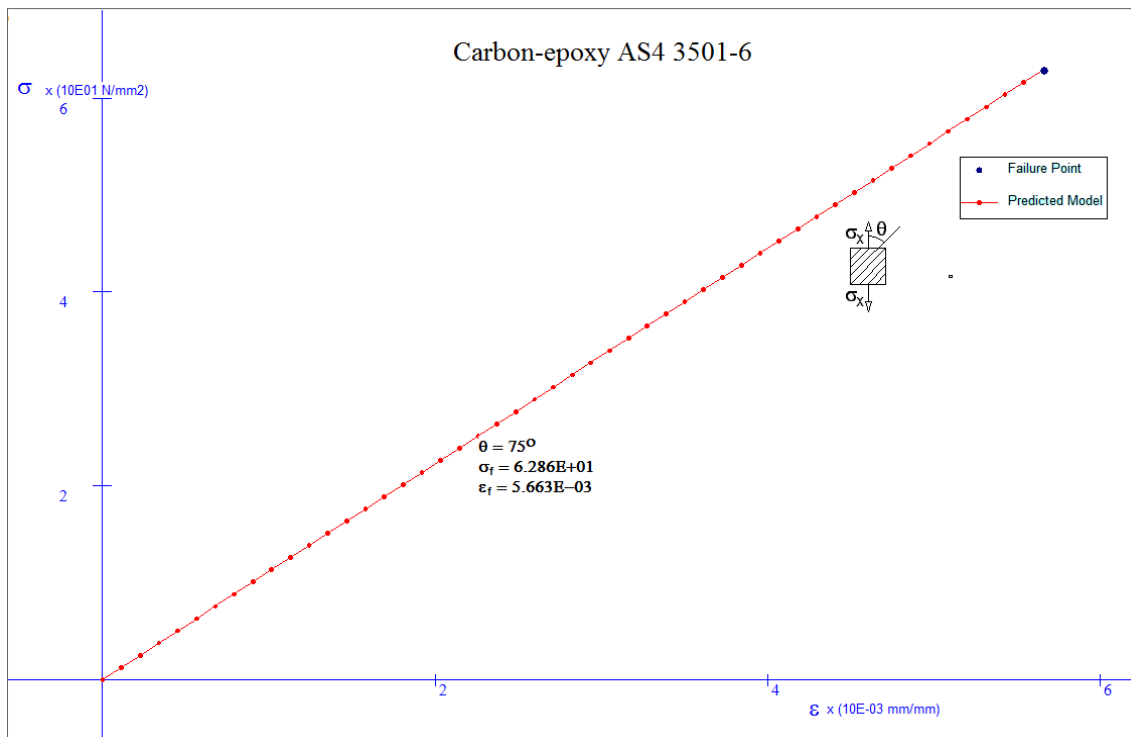
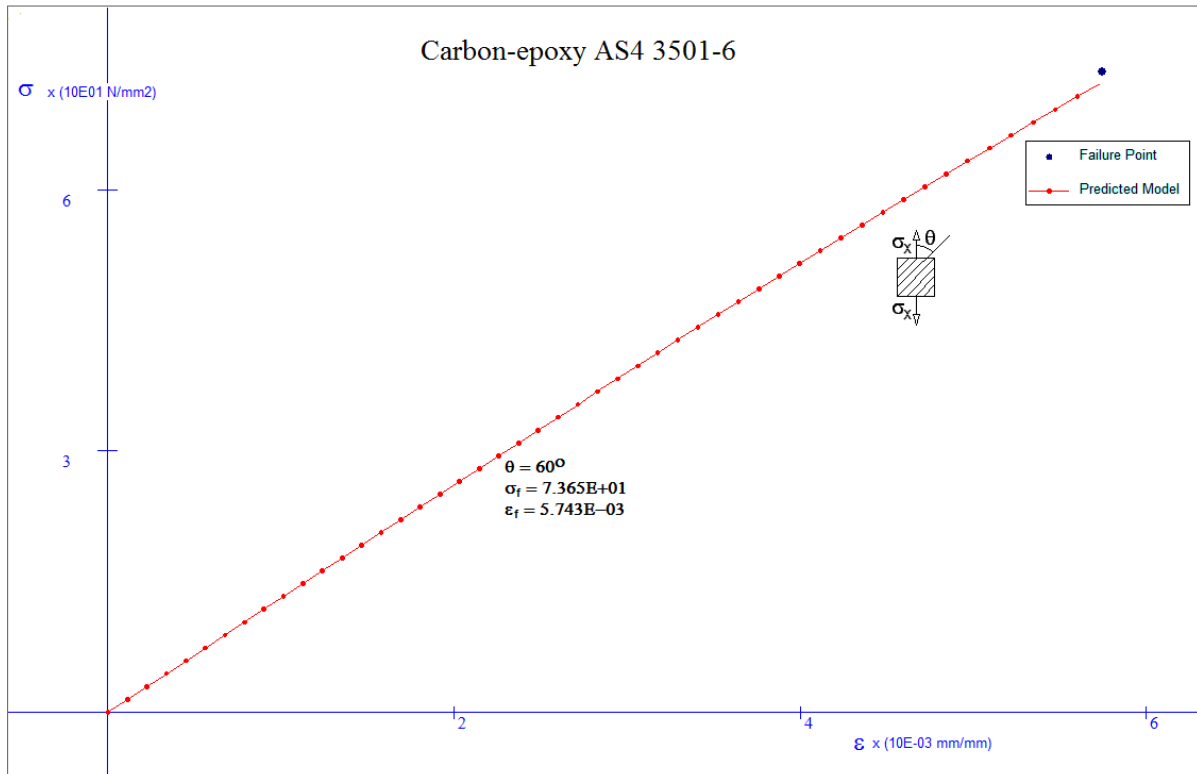
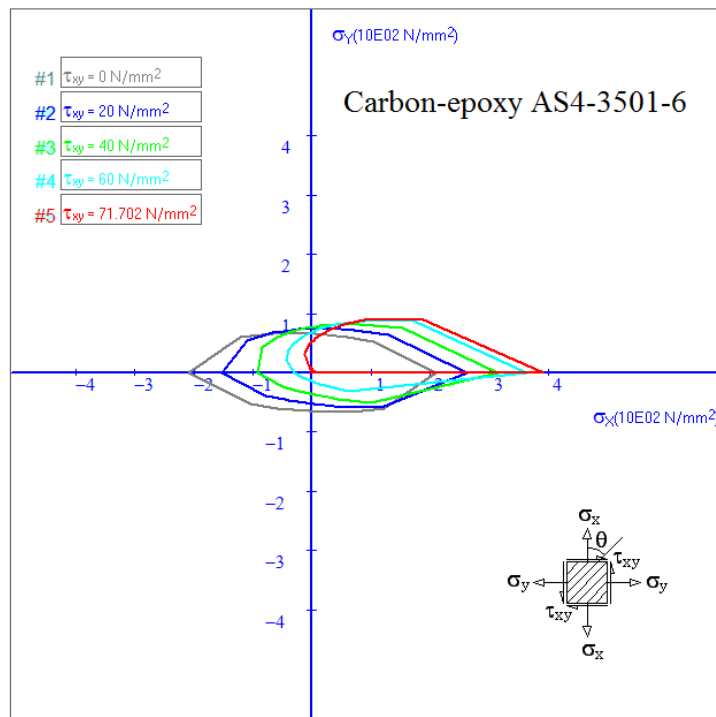


Figure 21: Stress-strain diagram for Carbon-Epoxy in the x-direction at  $\Theta=60$  degrees



**Figure 22: Stress-strain diagram for Carbon-Epoxy in the x-direction at  $\theta=75$  degrees**



**Figure 23: Failure envelopes for Carbon-Epoxy for various in-plane shear stresses at  $\theta=20$  degrees**

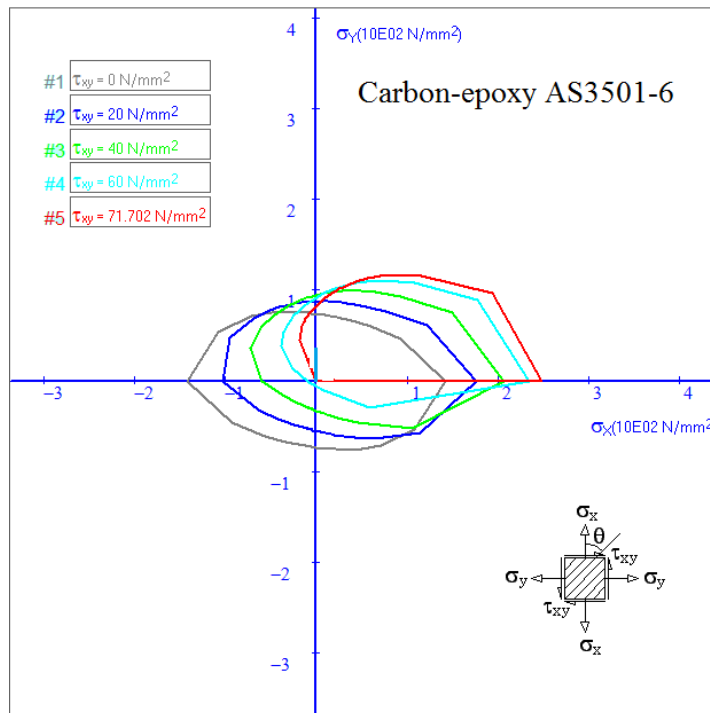


Figure 24: Failure envelopes for Carbon-Epoxy for various in-plane shear stresses at  $\theta=30$  degrees

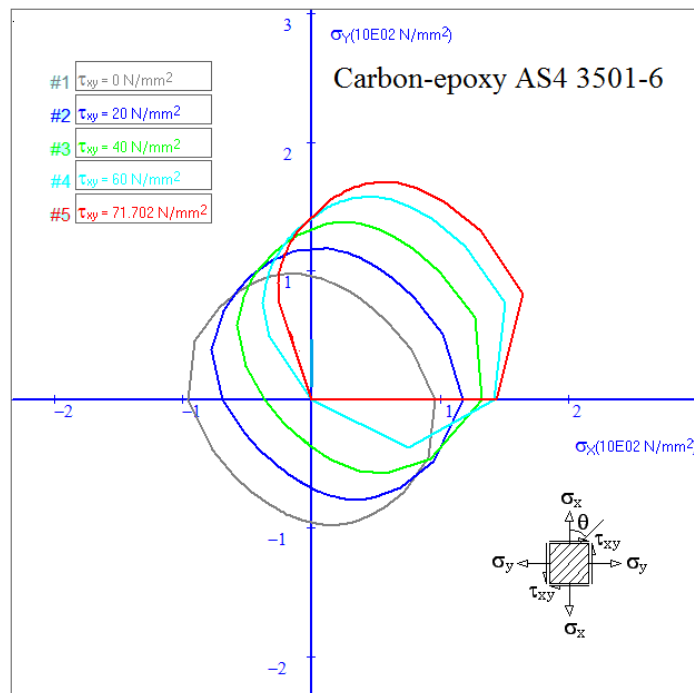


Figure 25: Failure envelopes for Carbon-Epoxy for various in-plane shear stresses at  $\theta=45$  degrees

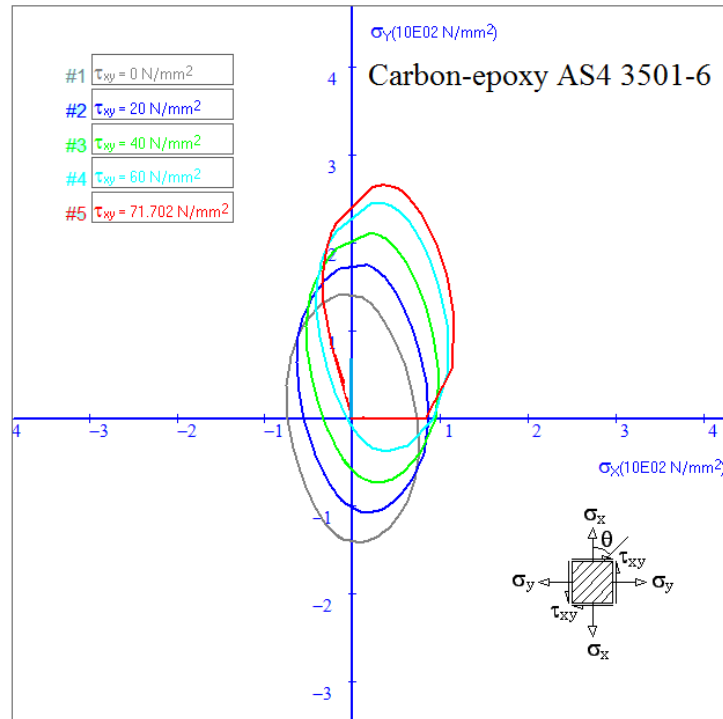


Figure 26: Failure envelopes for Carbon-Epoxy for various in-plane shear stresses at  $\theta=60$  degrees

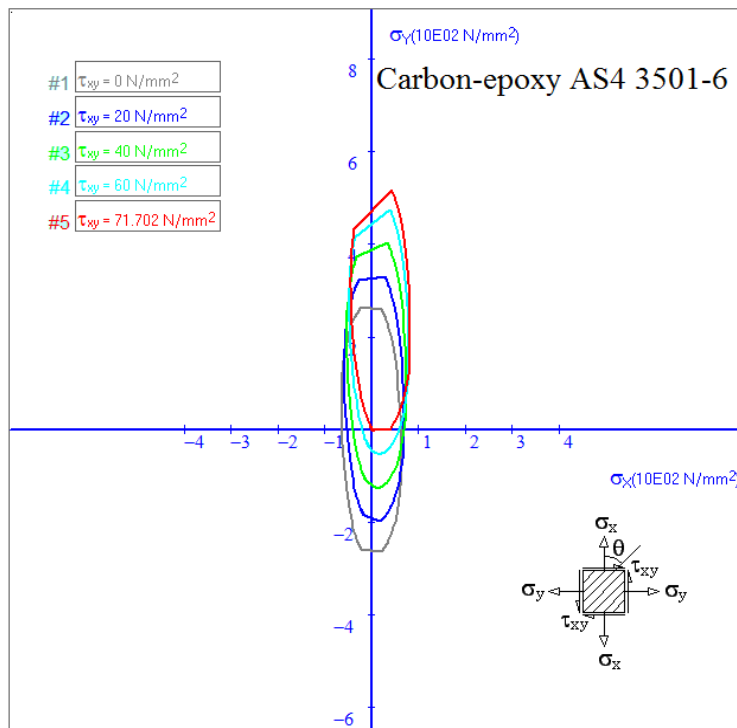


Figure 27: Failure envelopes for Carbon-Epoxy for various in-plane shear stresses at  $\theta=75$  degrees

## REFERENCES

- Abu-Farsakh, G. (1989). "New Material Models for Nonlinear Stress-strain Behaviour of Composite Materials". *Composites*, 20 (20), 349-360.
- Abu-Farsakh, G. A., and Abdel-Jawad, Y. A. (1994). "A New Failure Criterion for Nonlinear Composite Materials". *Journal of Composites Technology and Research (JCTRER)*, 17 (2), 138-145.
- Abu-Farsakh, G., and Almasri, A. (2011). "A Composite Finite Element to Predict Failure Progress in Composite Laminates Accounting for Nonlinear Material Properties". Accepted for Publication in: *Structural Control and Health Monitoring*.
- Cole, P. W., and Pipes, R. B. (1973). "Filamentary Composite Laminates Subjected to Biaxial Stress Fields". IIT Research Inst., Chicago, III, and Drexel University, Philadelphia, Pa., Air Force Flight Dynamics Lab. Technical Report AFFDL-TR-73 (June 1973).
- Donadon, V. M., de Almeida, S. F. M., Arbelo, M. A., and de Faria, A. R. A. (2009). "A Three-dimensional Ply Failure Model for Composite Structures". *Int. J. of Aerospace Engineerings*, 1-23.
- Donadon, V. M., Iannucci, L., Falzon, B. G., Hodgkinson, J. M., and de Almeida, S. F. M. (2008). "A Progressive Failure Model for Composite Laminates Subjected to Low Velocity Impact Damage". *Computers and Structures*, 86 (11-12), 1232-1252.
- Frost, S. R. (1990). "An Approximate Theory for Predicting the Moduli of Uni-directional Laminates with Non-linear Stress/Strain Behavior". *J. Composite Materials*, 24, 269-292.
- Gibson, R. F. (1994). *Principles of composite material mechanics*, McGraw-Hill, New York.
- Hashin, Z. (1979). "Analysis of Properties of Fiber Composites with Anisotropic Constituents". *ASME J. Appl. Mech.*, 46, 543-550.
- Hashin, Z. (1983). "Analysis of Composite Materials- A Survey". *ASME J. Appl. Mech.*, 50, 481-505.
- Hashin, Z., and Rosen, B. W. (1964). "The Elastic Moduli of Fiber-reinforced Materials". *ASME J. Appl. Mech.*, 12, 223-232.
- Jones, R. M. (1975). *Micromechanics of composite materials*, McGraw-Hill Scripta Book Company, New York.
- Soden, P. D., Hinton, M. J., and Kaddour, A. S. (1998). "Lamina Properties, Lay-up Configurations and Loading Conditions for a Range of Fiber-reinforced Composite Laminates". *Composite Science and Technology*, 58 (7), 1011-1022.
- Soden, P. D., Hinton, M. J., and Kaddour, A. S. (2002). "Biaxial Test Results for Strength and Deformation of a Range of E-glass and Carbon Fiber Reinforced Composite Laminates: Failure Exercise Benchmark Data". *Composite Science and Technology*, 62, 1489-1514.
- Sun, C. T., and Vaidya, R. S. (1994). "On Predicting Elastic Moduli and Plastic Flow in Composite Materials Using Micromechanics". *Proceedings of the 8<sup>th</sup> Technical Conference of the American Society for Composites (ASC)*, Cleveland, OH, USA, 841-850.
- Willis, J. R. (1977). "Bounds and Self-consistent Estimates for the Overall Moduli of Anisotropic Composites". *Journal of the Mechanics and Physics of Solids*, 25, 185-202.